IFSCC 2025 full paper (347)

"Skin Issues Management Under in Vitro Human Chronic Stress 3D Skin Equivalents Through Treatment With Ectoin: By Modulating the Glucocorticoid Receptor Chaperone HSP70-HSP90-Complexes"

Dailin Xu [1], Fan Chen [1], Yuqing Hu [1], Yijie Liu [1], and Yue Wu [1,*]

[1] In vitro research studio, Bloomage Biotechnology Corporation Limited, Shanghai, China

1. Introduction

The modern concept of stress traces back to Selye's book on General Adaptation Syndrome (GAS), which identified the hypothalamic-pituitary-adrenal (HPA) axis and sympathetic-adrenal-medullary (SAM) system as central orchestrators of stress responses. These evolutionarily conserved systems optimize survival through dynamic neurohormonal adjustments, acutely enhancing cognitive function, cardiovascular output, and immune surveillance [1]. At the molecular level, HPA activation initiates with hypothalamic corticotropin-releasing hormone (CRH) triggering anterior pituitary adrenocorticotropic hormone (ACTH) release, ultimately driving adrenal cortisol secretion —— the primary human glucocorticoid [2]. This endocrine cascade demonstrates remarkable duality: acute stress triggers transient cortisol (CORT) surges (recovery within 70 minutes post-exposure), providing adaptive benefits via enhanced gluconeogenesis and anti-inflammatory responses [3], whereas chronic stress (CS) disrupts homeostasis through flattened circadian CORT rhythms and glucocorticoid receptor (GR) desensitization [4]. The transition from adaptive to pathological states involves multiple mechanisms: 1) Paraventricular nucleus of hypothalamus/Arginine Vasopressin (PVN/AVP) ratio dysregulation [5], 2) 11β-hydroxysteroid dehydrogenase type 1 (11β-HSD1)-mediated tissue CORT activation [6], and 3) HSP70-HSP90-Complexes-mediated GR resistance[7].

The skin is continuously exposed to external stressors (UV radiation, pollution, temperature shifts) and internal triggers (nutritional deficits, medications, sleep deprivation), all recognized as central HPA axis activators [8]. In addition, the skin, as a neuroimmune interface, autonomously synthesizes CORT through localized HPA axis activation of cholesterol metabolism pathways [9]. Alarmingly, epidemiological studies reveal 68% of young adults (18-35 years) report CS manifestations, with 42% exhibiting stress-related dermatological conditions, with flattened CORT slopes correlating to 2.3-fold higher prevalence of eczema and psoriasis [10]. Chronic CORT secretion disrupts negative feedback regulation, causing cutaneous fragility, including disrupted skin barrier integrity (reduced corneodesmosome density [11], diminished stratum corneum lipids [12], granular layer atrophy, widened keratinocyte intercellular spaces

[13]), altered dermal texture (hyaluronic acid degradation[14], downregulated type I/III collagen expression [15]), and chronic inflammation (suppressed antimicrobial peptide production [16], immune cell hypoactivity[17], inflammatory senescence [18]). Systemically, CS correlates with alopecia areata [19], gut dysfunction [20], osteoporosis [21], Alzheimer's disease [22] as well as depression [23]. All of these cascading effects necessitate targeted therapeutic strategies.
Current preclinical models exhibit limitations in recapitulating human stress pathophysiology. Murine systems exhibit fundamental species disparities in GR distribution and stress response kinetics [24], while ethical constraints increasingly restrict animal experimentation. Clinical CORT measurements such as serum/saliva (for acute stress [25,26]) and hair and nail CORT content (chronic stress scores [27,28]), lack resolution for stressor heterogeneity across age distributions, socioeconomic strata, and individual neurobehavioral adaptability. This variability necessitates physiologically relevant in vitro human models for mechanistic studies. Reconstructed human skin equivalent (RHE) now enable controlled glucocorticoid exposure paradigms that recapitulate CS microenvironments while permitting real-time, quantifiable skin phenotyping. For example, Madhura et al. demonstrated dose-dependent cortisol effects on HA synthesis in human dermal equivalents, establishing quantifiable endpoints for therapeutic interventions [29].
Herein, we developed a 3D full-thickness RHE to simulate CS pathology through controlled CORT exposure, recapitulating glucocorticoid-mediated pathophysiological cascades: 1) Loosening of the stratum corneum and inhibition of lipid synthesis; 2) Reduced ex-pression of filaggrin in the granular layer, indicating incomplete differentiation; 3) Expansion of intercellular spaces and downregulated desmoglein in the spinous layer; 4) Disordered basal layer cells, with cytoplasmic red staining and nuclear condensation; 5) Dermal atrophy and reduced collagen synthesis. This platform demonstrates utility in screening stress-mitigating actives, with Ectoin showing marked anti-stress efficacy—specifically via modulation of HSP70-90 complexes. By bridging the technical gap in stress response, the system provides an ethical, human-relevant framework for testing stress-alleviating therapies and elucidating cutaneous glucocorticoid dynamics.

2. Materials and Methods

2.1. Materials

Cortisol standard solution was purchased from Sigma-Aldrich (St. Louis, MO, USA). Other reagents without specifically stated were from sigma-aladin.
The normal human dermal fibroblast (NHDF) and human epidermal keratinocyte (HEKn) were provided by American Type Culture Collection (ATCC) Center. Signed informed consent and ethical approval were obtained by the supplier.

2.2. Establishment of reconstructed full-thickness skin equivalent

The reconstructed full-thickness human skin equivalent is composed of normal human keratinocytes and human dermal fibroblasts that have been fused together via tissue engineering to generate a highly differentiated dermal-epidermal complex that is regularly utilized as an active screening model. The establishment of reconstructed full-thickness skin equivalents was carried out according to the Gangatirkar's protocol. Notably, 0.4 μg/ml cortisol were contained in the culture system (labeled maintenance medium) to suppot skin development. NHDF cells mixed with collagen were cultured to establish dermis. After collagen

lattice was formed, HEKn were seeded onto the surface of collagen lattice and media was changed every 2–3 days for the next 7 days. Then the skin equivalents were cultivated at an air-liquid interface for 8 days and media was changed every 2–3 days for the next 8 days. After cultured at air-liquid interface for 1 days to 7 days, another 0.2 μg/mL to 11.6 μg/mL cortisol were added into maintenance medium to simulate CS exposure until the culture period ended.

2.3. Histology and immunohistochemical analysis

At the end of the air-liquid cultivation, skin equivalents were fixed with 4% paraformaldehyde. Dehydration was carried out by gradient ethanol, followed by paraffin embedding. Sections were cut into slices of 5 μm and mounted onto the glass slides. After deparaffinized with methyl cyclohexane and rehydrated with decreasingly gradient ethanol, the tissue sections were stained with hematoxylin and eosin stain (H&E). Observation and photography were performed under a microscope.

For immunohistochemical analysis, skin equivalents were coated with O.C.T and cut into slices of 5 μm and mounted onto the glass slides. The sections were fixed with cold methyl alcohol for 15 min. BSA (5%) was added as a blocking solution and incubated for 1 h at room temperature. After that, DSG1, LN5, Ki67, COL1, FLG primary antibody, purchased from Abcam or Invitrogen, diluted by blocking solution were added separately and incubated overnight at 4^{o}C. On the following day, sections were washed with PBS and incubated with the corresponding secondary antibody for 1.5 h at room temperature, then covered with a mounting medium containing DAPI. Photos were taken under a fluorescence microscope. The mean fluorescence intensity of every photograph was analyzed using ImageJ software.

2.4. Quantitative PCR and Omics analysis

Transcriptomic profiling of in vitro RHE was conducted via RNA-seq. Total RNA was extracted, quality-controlled (Agilent 2100 Bioanalyzer, RIN $\geqslant$8), and enriched for mRNA through poly(A) selection or rRNA depletion. Strand-specific libraries were constructed (fragmented mRNA, cDNA synthesis, adapter ligation), validated by Qubit 2.0, Agilent 2100, and qRT-PCR. Libraries were sequenced on Illumina platforms using sequencing-by-synthesis. Bioinformatics analysis included raw data filtering (Trimmomatic), GRCh38 alignment (STAR), gene quantification (featureCounts), differential expression (FDR<0.05, |log2FC|>1), PCA, and functional enrichment (GO/KEGG).

2.5. Statistical analysis

The findings are presented as mean ± SD, with statistical significance being determined by P-values less than 0.05. With the use of Dunnett's post test and one-way analysis of variance, GraphPad 9.5.0 (GraphPad Software, San Diego, CA, U.S.A.) was used.

3. Results

3.1. Assessment of reconstructed human skin equivalent (RHE) response to cortisol

To model chronic stress (CS) -induced skin pathology, physiological stress dose of cortisol (CORT) was added into maintenance medium of RHE. Untreated RHE (group NC) maintained native epidermal stratification, including the stratum corneum (SC), stratum granulosum (SG), stratum spinosum (SS), vertically oriented stratum basal layer (SB), and a collagen-rich dermal layer (Figure 1A).

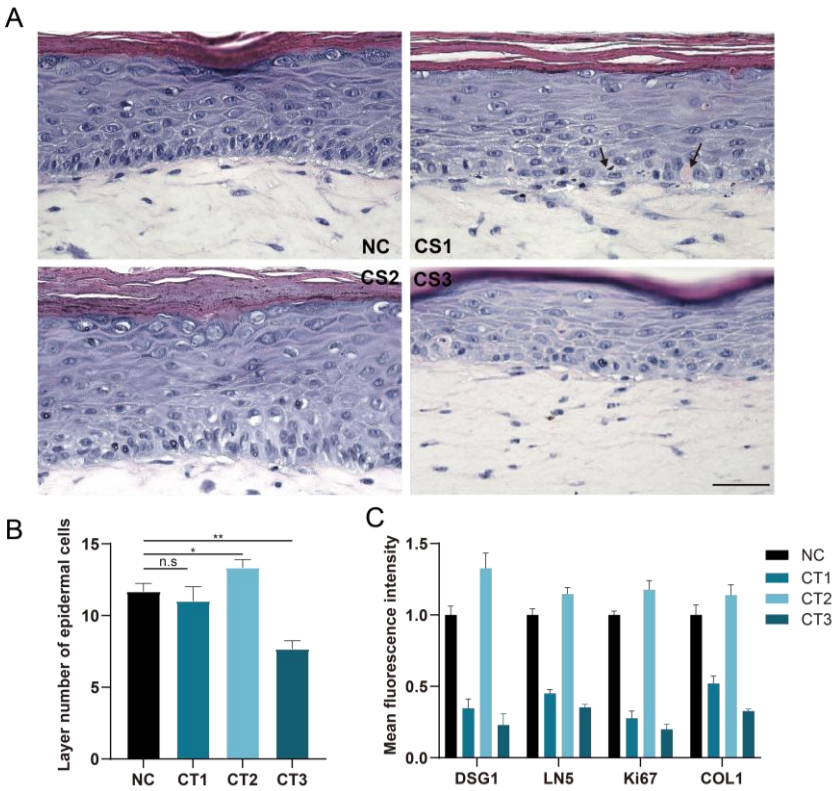

Figure 1. Assessment of RHE response to CORT. Another 0.2 µg/mL CORT was added into maintenance medium for 2 days culture of group CS1, 0.8 µg/mL CORT in 4 days treatment for group CS2, and 11.6 µg/mL CORT in 7 days treatment for CS3. (A) H&E staining in re-structured full-thickness skin equivalents at 400× magnification (scale bar: 50 µm). And black arrows represent cytoplasmic red staining, and the white arrows represent nuclear condensation. (B) Layer number of epidermal cells of CS1, CS2, CS3. (C) DSG1, LN5, Ki67, COL1 were measured by immunohistochemical analysis. The following is how statistical significance is expressed: P < 0.05 for *, 0.01% for **

Following low dose of CORT exposure for 2 days (Group CS2), RHE exhibited hyperproliferation with increased epidermal stratification (Figure 1B) and upregulated biomarkers including desmoglein 1 (DSG1), laminin-5 (LN5), proliferative marker Ki67, and collagen I (COL1) density (Figure 1C). In contrast, prolonged medium dose of CORT exposure for 4 days (Group CS1) induced pathological remodeling characterized by almost disappeared SG, intercellular junction disruption (downgulated DSG1), loosened dermal-epidermis junctions (downgulated LN5), basal cell flattening with cytoplasmic red staining and nuclear condensation, and downgulated Ki67 and COL1, mirroring clinical CS phenotypes. Notably, 30 folds of physiological CORT exposure over 7 days (Group CS3) caused cytotoxic differentiation arrest (≤9 epidermis layers), reflecting destructive stimulation rather than chronic stress mimicry. These results demonstrate dose- and duration-dependent CORT effects, with CS1 conditions successfully replicating hallmark features of stress-mediated skin dysfunction while distinguishing pathological mechanisms from acute adaptive responses or cytotoxic damage.

3.2. Chronic stress-driven glucocorticoid receptor (GR) activation modulates mRNA levels of genes with functional roles in RHE.

Identifying glucocorticoid actions in human skin equivalents provides critical insights into the long-term physiological and behavior consequences of CS exposure, while enabling prediction

of stress-associated pathologies ranging from cutaneous barrier dysfunction to severe psycho-pathologies. Therefore, total RNA was then prepared from 3 independent CS treatment RHE, and subjected to RNA-Seq analysis to identify the GR-regulated transcriptome (Table 1 and Figure 2A).

Table 1. GR-Target Genes Identified Using RNA-Seq Analysis in CS RHE

Gene	Fold change	Gene	Fold change	Gene	Fold change
SLC25A41	34.00	*TCEA1P2*	2.02	*CYP2T1P*	0.36
MIR4432HG	29.37	*RGPD5*	2.00	*SERF1B*	0.34
TRIM31-AS1	24.52	*FRMPD1*	0.49	*SLC16A10*	0.32
PRODH	19.59	*GALNT16*	0.49	*SLC46A2*	0.31
BOLA2B	18.89	*VWCE*	0.47	*ELF5*	0.31
PATL2	9.66	*DEGS2*	0.47	*NOMO3*	0.31
LMCD1-AS1	8.43	*TXLNB*	0.47	*ADCY1*	0.30
QRFP	8.04	*SLC19A3*	0.47	*UPK1A*	0.29
NPIPB10P	6.40	*IGSF22*	0.46	*SH3GL3*	0.24
LYL1	6.32	*HYAL4*	0.44	*ZNF497-AS1*	0.23
DHRSX	5.49	*C1QTNF7*	0.44	*OMG*	0.23
CPVL-AS2	5.00	*COPG2IT1*	0.43	*IL13RA2*	0.21
PILRA	3.81	*SERPINA12*	0.42	*TBC1D3K*	0.18
SMG1P2	2.54	*LINC02159*	0.42	*THEGL*	0.15
FOSB	2.40	*STUM*	0.41	*FGF17*	0.08
PPP2R3B	2.38	*BAALC-AS2*	0.40	*PRODHLP*	0.08
PCLAF	2.37	*NLGN4X*	0.38	*MGARP*	0.05
KIF21B	2.23	*SLC1A2*	0.38	*LINC02666*	0.04
MXRA7P1	2.08	*DNAH10OS*	0.38	*DEFB103A*	0.04

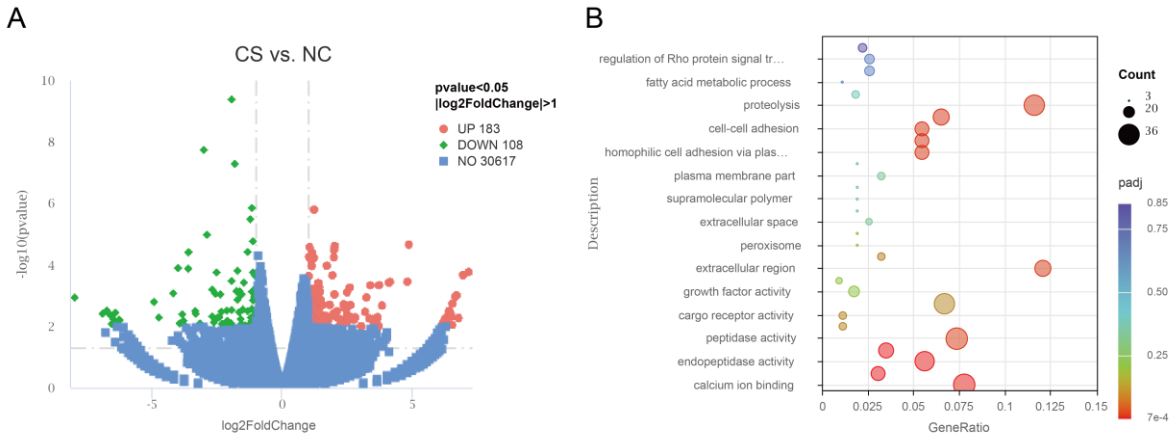

Figure 2. Chronic stress-driven GR activation modulates mRNA levels of genes with functional roles in RHE. (A) Volcano plot showing differences in mRNA levels of all genes in the CS exposure RHE vs. NC. GR-modulated genes are labeled in table 1. (B) Gene ontology (GO) biological process analysis of GR-modulated genes. GO analysis was performed using WebGestalt (WEB-based Gene SeT AnaLysis Toolkit). The x-axis shows genes annotated to GO terms versus total; y-axis lists GO terms. Dot size indicates annotated genes per term, with color gradient (red-purple) showing enrichment significance. Padj means adjusted p value.

Our findings identified a number of genes and pathways potentially governing cutaneous responsiveness to glucocorticoids, with particular relevance to skin barrier integrity and functional adaptations. RNA-seq analysis identified 291 differentially expressed genes (DEGs, DESeq2 $p \leq 0.05$), with genes exhibiting >2-fold changes tabulated. Notably, DEFB103A,

IL13RA2, and NOMO3—critical regulators of immune homeostasis, antimicrobial defense, and anti-inflammatory responses—were significantly downregulated, suggesting heightened risks of CS-associated pathologies such as atopic dermatitis and cutaneous ulceration. Concurrent suppression of epidermal proliferation, differentiation and lipid metabolism modulators (LINC02666, ELF5, DEGS2, UPK1A) corroborated histopathological observations in Figure 1A. Furthermore, reduced expression of SLC transporters (SLC16A10, SLC19A2, SLC19A3)—key mediators of metabolic regulation and epidermal energy homeostasis—indicates impaired detoxification capacity and attenuated stress adaptation, potentially predisposing to delayed tissue repair and metabolic dermatoses. GO-term enrichment analysis of GR-modulated DEGs revealed significant enrichment for proteolysis, extracellular region, calcium ion binding, cell adhesion (Figure 2B). These transcriptional signatures collectively delineate molecular pathways linking chronic glucocorticoid exposure to cutaneous dysfunction.

3.3. Ectoin impacts under CS on Skin barrier fuctions and texture

As the body's foremost protective barrier, the skin protects against exogenous chemical and physical intrusion, participates in internal metabolism, and maintains internal equilibrium.

Histopathological evaluation revealed distinct epidermal remodeling under CS. RHE in NC group maintained a well-stratified, fully differentiated epidermis, whereas physiological CORT exposure under CS severely compromised epidermal integrity, evidenced by granular layer atrophy (near-complete disappearance), expanded intercellular spaces in SG, disordered basal cell alignment, and apoptotic morphology (Figure 3A), indicating disrupted regenerative capacity. Ectoin treatment counteracted these structural aberrations to some extent.

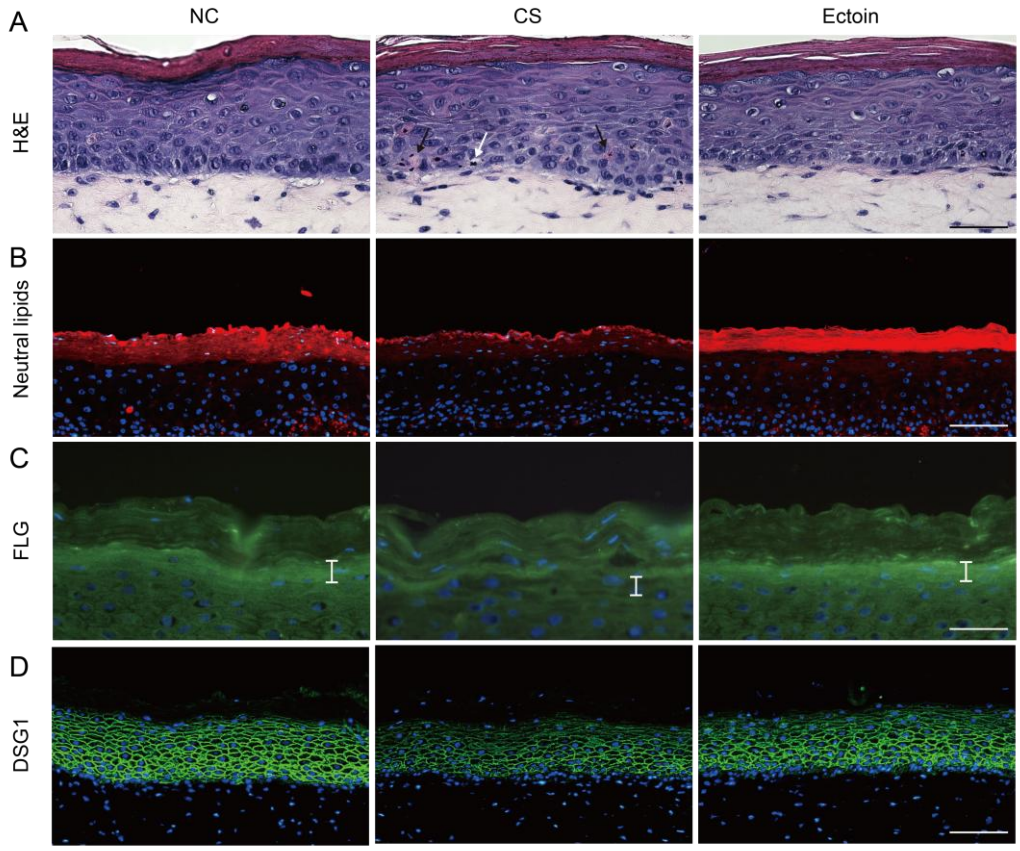

Immunohistochemical profiling further delineated barrier-related biomarkers. The stratum corneum, critical for permeability barrier function via intercellular lipids (ceramides, cholesterol,

free fatty acids), exhibited loosened compaction and suppressed lipid synthesis under CS, which were reversed by Ectoin treatmet (Figure 3B). Filaggrin (FLG), essential for cornified envelope formation and predominantly localized to SG, showed marked downregulation in CS-exposed RHE, correlating with the histologically observed granular layer loss. Ectoin restored FLG expression, normalizing terminal differentiation (Figure 3C).

Epidermal intercellular junctions comprise three primary types: corneodesmosomes (SC, regulating desquamation), tight junctions (SG), and desmosomes (SS and SB). CS induced expansion of intercellular spaces in Figure 3A, correlated with significant DSG1 downregulation, while Ectoin treatment attenuated DSG1 degradation (Figure 3D). Notably, nuclear retention in SC under CS revealed disordered programmed cell death, indicating defective keratinocyte differentiation.

Basal cell dynamics, assessed via Ki67, demonstrated CS-induced apoptosis, likely driven by chronic inflammation [17], with Ectoin partly preserving proliferative capacity (Figure 3E). At the dermal-epidermal junction (DEJ), LN5 suppression under CS compromised dermal support and nutrient transport, counteracted by Ectoin-mediated anti-stress effects (Figure 3F).

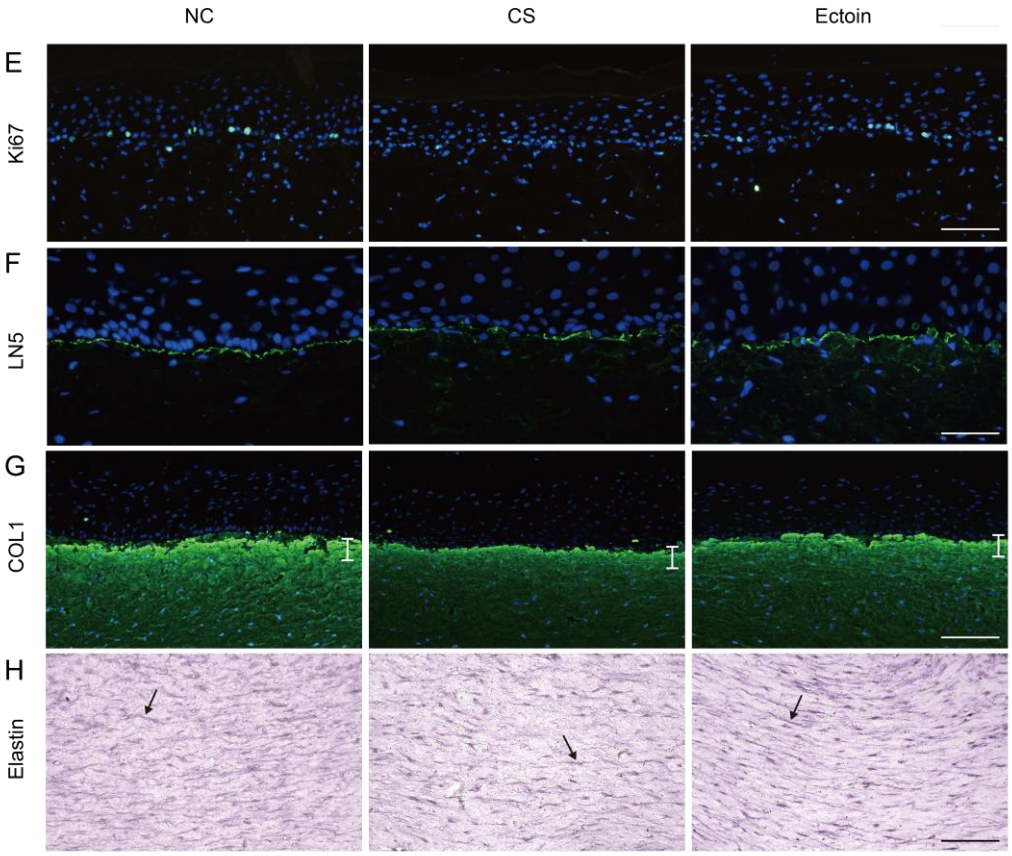

Figure 3. Ectoin impacts under CS on Skin Health. Treatment of RHE were either vehicle (labeled NC) or CORT (CS1 conditions) with or without Ectoin (0.5 mg/mL) for 4 days. (A) H&E staining, and black arrows represent cytoplasmic red staining, and the white arrows represent nuclear condensation. (B) Nile red staining with neutral lipids in SC. (C) FLG, (D) DSG1, (E) Ki67, (F) LN5, (G) COL1 were measured by immunohistochemical analysis. White truncated positionin in (C) reflects the main expression region of FLG is SG, while in (G) reflects the main secretion region of COL1 is fibroblasts near the DEJ (i.e., mastoid layer cells). (H) Aldehyde fuchsin staining with elastic fibers in dermis, and the black arrows show the elastin fibers. H&E, FLG, LN5 were shot at 400× magnification (scale bar: 50 μm) and Neutral lipids, DSG1, Ki67, COL1, Elastin were shot at 200× magnification (scale bar: 100 μm).

Stress-accelerated skin textural alterations mechanistically mirror natural aging, with clinical validation from irreversible dermal atrophy observed in chronic glucocorticoid-treated patients. These changes primarily stem from COL1 and elastin dysregulation—structural pillars of mechanical resilience. Papillary fibroblasts at the DEJ, which exhibit high collagen-secretory activity, showed downregulation of COL1 under CS. Ectoin treatment reactivated COL1 synthesis, restoring fibroblast biosynthetic capacity (Figure 3G). Elastin, synthesized predominantly during fetal/neonatal development with lifelong persistence, undergoes progressive network disorganization under mechanical and stress insults. Elastic fiber density declined under CS, predisposing to skin laxity and rhytides. Ectoin attenuated CS-induced elastolysis, preserving elastic fiber integrity versus untreated controls (Figure 3H).
All results showed Ectoin confers multifaceted protection in CS-exposed RHE, these coordinated mechanisms underscore its therapeutic potential in stress.

3.4. Mechanism Exploration of Ectoin on anti-CS therapy

Under physiological conditions, the GR forms cytoplasmic complexes with chaperone proteins (HSP70, HSP90), p23, and immunophilins (FKBP51/FKBP52), rendering it transcriptionally inactive [30]. Glucocorticoid (GC) binding triggers GR nuclear translocation, where it modulates metabolic, immune, and inflammatory pathways through transactivation or transrepression mechanisms.
Ectoin, previously shown to upregulate HSP70 and HSP70B' in keratinocytes with anti-inflammatory effects [31], was investigated for HSP90 regulation under CS. Our data demonstrated CS-induced HSP90 proteolysis which was attenuated by Ectoin treatmet (Figure 4A). This aligns with prior findings of Ectoin-mediated suppression of GR phosphorylation in stressed fibroblasts, suggesting a coordinated chaperone stabilization mechanism [32].

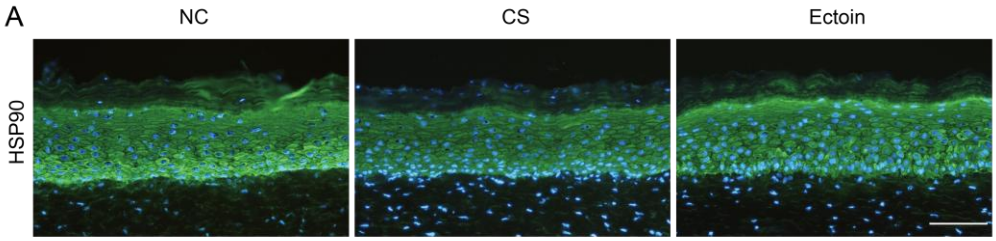

Figure 4. Ectoin moderated HSP90 expression under CS on RHE. Treatment of RHE were either vehicle (labeled NC) or CORT (CS1 conditions) with or without Ectoin (0.5 mg/mL) for 4 days. (A) HSP90 expression was measured by immunohistochemical, and was shot at 200× magnification (scale bar: 100 μm).

4. Discussion

Glucocorticoids (GCs) serve as critical lipid-derived hormones regulating stress adaptation, metabolic homeostasis, and immune modulation. Dysregulation of GC signaling underlies systemic pathologies, exemplified by the cardiovascular and immunological complications observed in Cushing's syndrome (Hypercortisolism) and Addison's disease (Cortisol deficiency).

Cortisol exhibits context-dependent bioactivity shaped by dosage, exposure duration, tissue-specific GR density, and cellular signaling milieu. Physiological cortisol secretion follows a circadian rhythm peaking at 8:00 AM and reaching its nadir by midnight. Chronic stress disrupts

this pulsatility, characterized by flattened diurnal cortisol slopes and diminished negative feedback—a pattern mirroring circadian dysregulation observed in dermatological deterioration[33]. The heterogeneity of stress responses is evident in cortisol fluctuations across species and conditions: human plasma cortisol increases 1.2–1.4-fold post-exercise [26], compared to 100-fold corticosterone (Cortisol equivalent to rodents) spikes in water-avoidance-stressed rodents [34]. Salivary cortisol rises 1.36-fold following the Trier Social Stress Test (TSST) [35] and 3.3-fold in smokers with chronic periodontitis in another test [36]. As both a sensor and effector of stress, the skin autonomously generates cortisol via 11β-HSD1-mediated activation of cortisone, positioning RHE as a quantifiable model for chronic stress interrogation.

Transcriptomic profiling delineated GR-mediated genomic reprogramming spanning seven functional domains—immunoinflammatory modulation (DEFB103A, IL13RA2), epidermal barrier regulation (ELF5, DEGS2), neurosensory adaptation (OMG, NLGN4X), proliferative control (FOSB, PCLAF), extracellular matrix remodeling (FGF17, VWCE), metabolic/redox homeostasis (THEGL, SLC16A10), and cellular trafficking (PPP2R3B). These pan-tissue effects underscore chronic stress as a systemic homeostatic disruptor, with cutaneous manifestations reflecting underlying GR-driven equilibrium collapse. Therapeutic strategies targeting GR signaling may involve modulation of 11β-HSD1, enhancement of hepatic cortisol clearance, or chaperone-mediated GR regulation. The latter requires sequential HSP70/40 priming, HSP90/HOP complex assembly, and FKBP51/52-dependent cytosolic retention or nuclear translocation.

Our findings align with prior evidence that Ectoin, a halophile-derived amino acid derivative, attenuates GR signaling through dual stabilization of HSP70 and HSP90, thereby inhibiting receptor phosphorylation. This chaperone-centric mechanism likely contributes to its efficacy in mitigating stress-induced epidermal atrophy, barrier dysfunction, and dermal matrix degradation. Future studies should delineate tissue-specific GR interactomes to optimize therapeutic targeting of stress-exacerbated dermatoses, bridging molecular chaperone dynamics with clinical phenotype resolution.

5. Conclusion

Chronic stress disrupts the delicate equilibrium of human stress adaptation, enabling glucocorticoids (GCs) to exert predominant deleterious effects that drive systemic endocrine dysregulation, epidermal barrier compromise, and dermal textural alterations. Our development of a chronically stressed human skin equivalent—exhibiting high reproducibility, scalable production capacity, and pathophysiological fidelity to human glucocorticoid-induced dermatopathies—provides a translational platform for mechanistic interrogation and therapeutic innovation. By demonstrating Ectoin's capacity to modulate molecular chaperones HSP70 and HSP90 within the GC signaling axis, this work illuminates its therapeutic potential in mitigating stress-aggravated cutaneous dysfunction, highlighting its utility for preclinical validation of stress-targeted dermatological interventions.

Reference

[1] Vitellius G, Trabado S, Bouligand J, Delemer B and Lombès M 2018 Pathophysiology of glucocorticoid signaling *Ann Endocrinol (Paris)* 79 98–106
[2] Cruz-Topete D and Cidlowski J A 2015 One hormone, two actions: anti- and pro-inflammatory effects of glucocorticoids *NeuroImmunoModulation* 22 20–32
[3] Jia W Y and Zhang J %J W journal of clinical cases 2022 Effects of glucocorticoids on leukocytes: genomic and non-genomic mechanisms 10 7187–94
[4] Russell G and Lightman S 2019 The human stress response *Nat Rev Endocrinol* 15 525–34
[5] Ma X M, Levy A and Lightman S L 1997 Emergence of an isolated arginine vasopressin (AVP) response to stress after repeated restraint: a study of both AVP and corticotropin-releasing hormone messenger ribonucleic acid (RNA) and heteronuclear RNA *Endocrinology* 138 4351–7

[6] Cirillo N and Prime S S 2011 Keratinocytes synthesize and activate cortisol *J. Cell. Biochem.* 112 1499–505
[7] Wang R Y, Noddings C M, Kirschke E, Myasnikov A G, Johnson J L and Agard D A 2022 Structure of Hsp90-Hsp70-hop-GR reveals the Hsp90 client-loading mechanism *Nature* 601 460–4
[8] Celebi Sözener Z, Cevhertas L, Nadeau K, Akdis M and Akdis C A 2020 Environmental factors in epithelial barrier dysfunction *J. Allergy Clin. Immunol.* 145 1517–28
[9] Itoi-Ochi S, Terao M, Murota H and Katayama I 2016 Local corticosterone activation by 11beta-hydroxysteroid dehydrogenase 1 in keratinocytes: the role in narrow-band UVB-induced dermatitis *Derm.-endocrinol.* 8 e1119958–e1119958
[10] National Institute of Mental Health. 2022 Stress Survey
[11] Kim B J, Lee N R, Lee C H, Lee Y B, Choe S J, Lee S, Hwang H J, Kim E, Lavery G G, Shin K O, Park K and Choi E H 2021 Increased expression of 11β-hydroxysteroid dehydrogenase type 1 contributes to epidermal permeability barrier dysfunction in aged skin *Int. J. Mol. Sci.* 22
[12] Sheu H, Lee J Y, Kuo K and Tsai J 1998 Permeability barrier abnormality of hairless mouse epidermis after topical corticosteroid: characterization of stratum corneum lipids by ruthenium tetroxide staining and high‐performance thin‐layer chromatography *J. Dermatol.* 25 281–9
[13] Sheu H, Tai C, Kuo K, Yu H and Chai C 1991 Modulation of epidermal terminal differentiation in patients after long‐term topical corticosteroids *J. Dermatol.* 18 454–64
[14] Gebhardt C, Averbeck M, Diedenhofen N, Willenberg A, Anderegg U, Sleeman J P and Simon J C 2010 Dermal hyaluronan is rapidly reduced by topical treatment with glucocorticoids *J. Invest. Dermatol.* 130 141–9
[15] Nuutinen P, Riekki R, Parikka M, Salo T, Autio P, Risteli J and Oikarinen A 2003 Modulation of collagen synthesis and mRNA by continuous and intermittent use of topical hydrocortisone in human skin *Brit. J. Dermatol.* 148 39–45
[16] Martin-Ezquerra G, Man M Q, Hupe M, Rodriguez-Martin M, Youm J K, Trullas C, Mackenzie D S, Radek K A, Holleran W M and Elias P M 2011 Psychological stress regulates antimicrobial peptide expression by both glucocorticoid and β-adrenergic mechanisms *Eur J Dermatol* 21 Suppl 2 48–51
[17] Cain D W and Cidlowski J A 2017 Immune regulation by glucocorticoids *Nat. Rev. Immunol.* 17 233–47
[18] Østergaard L, Jørgensen M B and Knudsen G M 2018 Low on energy? An energy supply-demand perspective on stress and depression *Neurosci. Biobehav. Rev.* 94 248–70
[19] Choi S, Zhang B, Ma S, Gonzalez-Celeiro M, Stein D, Jin X, Kim S T, Kang Y-L, Besnard A, Rezza A, Grisanti L, Buenrostro J D, Rendl M, Nahrendorf M, Sahay A and Hsu Y-C 2021 Corticosterone inhibits GAS6 to govern hair follicle stem-cell quiescence *Nature* 592 428-,
[20] Varanoske A N, McClung H L, Sepowitz J J, Halagarda C J, Farina E K, Berryman C E, Lieberman H R, McClung J P, Pasiakos S M and Philip Karl J 2022 Stress and the gut-brain axis: cognitive performance, mood state, and biomarkers of blood-brain barrier and intestinal permeability following severe physical and psychological stress *Brain Behav Immun* 101 383–93
[21] Adler R A 2019 Glucocorticoid-induced osteoporosis: management challenges in older patients *J. Clin. Densitom.* 22 20–4
[22] Ouanes S and Popp J 2019 High cortisol and the risk of dementia and alzheimer's disease: a review of the literature *Front. Aging Neurosci.* 11
[23] Kamin H S and Kertes D A 2017 Cortisol and DHEA in development and psychopathology *Horm Behav* 89 69–85
[24] Sarapultsev A, Komelkova M, Lookin O, Khatsko S, Gusev E, Trofimov A, Tokay T and Hu D 2024 Rat models in post-traumatic stress disorder research: strengths, limitations, and implications for translational studies *Pathophysiol.: Off. J. Int. Soc. Pathophysiol.* 31 709–60
[25] Chojnowska S, Ptaszyńska-Sarosiek I, Kępka A, Knaś M and Waszkiewicz N 2021 Salivary biomarkers of stress, anxiety and depression *J Clin Med* 10
[26] Schedlowski M, Wiechert D, Wagner T O and Tewes U 1992 Acute psychological stress increases plasma levels of cortisol, prolactin and TSH *Life Sci* 50 1201–5
[27] Janssens H, Clays E, Fiers T, Verstraete A G, de Bacquer D and Braeckman L 2017 Hair cortisol in relation to job stress and depressive symptoms *Occup Med (L.)* 67 114–20
[28] Davison B, Singh G R, Oguoma V M and McFarlane J 2020 Fingernail cortisol as a marker of chronic stress exposure in indigenous and non-indigenous young adults *Ann. Ny. Acad. Sci.* 23 298–307
[29] Deshpande M, Papp S, Schaffer L and Pouyani T 2016 Hydrocortisone effect on hyaluronate synthesis in a self-assembled human dermal equivalent *J Tissue Eng Regen Med* 10 E316-e326
[30] de Guia R M 2020 9 Stress, glucocorticoid signaling pathway, and metabolic disorders *Diabetes Metab Syndr* 14 1273–80
[31] Buommino E, Schiraldi C, Baroni A, Paoletti I, Lamberti M, De Rosa M and Tufano M A 2005 Ectoine from halophilic microorganisms induces the expression of hsp70 and hsp70B' in human keratinocytes modulating the proinflammatory response *Cell Stress Chaperones* 10 197–203
[32] Xu D and Wu Y 2024 Ectoin attenuates cortisone‐induced skin issues by suppression GR signaling and the UVB‐induced overexpression of 11β‐HSD1 *J. Cosmet. Dermatol.* 23 4303–14
[33] Vegas O, Poligone B, Blackcloud P, Gilmore E S, VanBuskirk J, Ritchlin C T, Pentland A P, Walter S A, Nousari Y and Tausk F 2018 Chronic social stress ameliorates psoriasiform dermatitis through upregulation of the hypothalamic-pituitary-adrenal axis *Brain Behav. Immun.* 68 238–47
[34] Takada M, Nishida K, Kataoka-Kato A, Gondo Y, Ishikawa H, Suda K, Kawai M, Hoshi R, Watanabe O, Igarashi T, Kuwano Y, Miyazaki K and Rokutan K 2016 Probiotic lactobacillus casei strain shirota relieves stress-associated symptoms by modulating the gut-brain interaction in human and animal models *Neurogastroenterol Motil* 28 1027–36
[35] Ney L, Stone C, Nichols D, Felmingham K, Bruno R and Matthews A 2021 Endocannabinoid reactivity to acute stress: investigation of the relationship between salivary and plasma levels *Biol. Psychol.* 159 108022
[36] Zhang H, Chen B, Pan C and Zhang A 2021 To evaluate the serum cortisol, salivary cortisol, and serum interleukin-1 B level in patients of chronic periodontitis with smoking and stress and without smoking and stress *Medicine (Baltimore)* 100 e26757